Two-Dimensional XY Ferromagnet Induced by Long-Range Interaction

Tianning Xiao^{1†}, Dingyun Yao^{1†}, Chao Zhang^{1,2*}, Zhijie Fan^{1,3,4*}, and Youjin Deng^{1,3,4*}

 ¹Hefei National Research Center for Physical Sciences at the Microscale and School of Physical Sciences, University of Science and Technology of China, Hefei 230026, China
 ²Department of Physics, Anhui Normal University, Wuhu 241000, China
 ³Hefei National Laboratory, University of Science and Technology of China, Hefei 230088, China
 ⁴Shanghai Research Center for Quantum Science and Chinese Academy of
 Sciences Center for Excellence in Quantum Information and Quantum Physics,
 University of Science and Technology of China, Shanghai 201315, China

(Received 18 April 2025; accepted manuscript online 29 May 2025)

The crossover between short-range and long-range (LR) universal behaviors remains a central theme in the physics of LR interacting systems. The competition between LR coupling and the Berezinskii–Kosterlitz–Thouless mechanism makes the problem more subtle and less understood in the two-dimensional (2D) XY model, a cornerstone for investigating low-dimensional phenomena and their implications in quantum computation. We study the 2D XY model with algebraically decaying interaction $\sim 1/r^{2+\sigma}$. Utilizing an advanced update strategy, we conduct LR Monte Carlo simulations of the model up to a linear size of L=8192. Our results demonstrate continuous phase transitions into a ferromagnetic phase for $\sigma < 2$, which exhibit the simultaneous emergence of a long-ranged order and a power-law decaying correlation function due to the Goldstone mode. Furthermore, we find logarithmic scaling behaviors in the low-temperature phase at $\sigma=2$. The observed scaling behaviors in the low-temperature phase for $\sigma \leq 2$ agree with our theoretical analysis. Our findings request further theoretical understanding and can be of practical application in cutting-edge experiments like Rydberg atom arrays.

DOI: 10.1088/0256-307X/42/7/070002

1. Introduction. Long-range (LR) interacting systems have been studied in statistical and condensed matter physics for decades, unveiling a range of exotic physical phenomena. [1-3] This interest has recently intensified, driven by the experimental realizations of such systems in atomic, molecular, and optical (AMO) setups. [4–10] In particular, the two-dimensional (2D) XY model with LR interactions has gained notable attention. [11-14] Without LR interactions, the model undergoes the celebrated Berezinskii-Kosterlitz-Thouless (BKT) transition driven by topological defects^[15] and serves as a fundamental cornerstone for understanding low-dimensional superfluidity [16] and superconductivity. [17-19] Upon incorporating LR interactions, however, it becomes a pivotal framework for exploring the complex interplay between LR interactions and the BKT mechanism. [15] Most importantly, recent implementations of the model in trapped ion setups and Rydberg systems demonstrate its significance in quantum computation. [10,13,14]

The XY model belongs to the classical $O(\mathcal{N})$ spin models with $\mathcal{N}=2$. The d-dimensional LR $O(\mathcal{N})$ spin model with power-law decaying $\sim 1/r^{d+\sigma}$ interactions has been extensively investigated, particularly regarding the renormalization group (RG) relevance of the LR interactions. [20–27] In such systems, a threshold σ_* sep-

CSTR: 32039.14.0256-307X.42.7.070002

arates the LR and short-range (SR) critical behaviors. For $\sigma > \sigma_*$, the system is in the same universality class as its nearest-neighbor (NN) counterpart, while for $\sigma \leq \sigma_*$, the LR interactions become relevant, yielding distinct critical properties. [21-23] The value of σ_* was first obtained in the seminal paper of Fisher et al., [21] where a second-order ϵ -expansion approach suggests $\sigma_* = 2$. Later, a new threshold $\sigma_* = 2 - \eta_{\rm SR}$ was proposed by Sak, [22] currently known as Sak's criterion, where $\eta_{\rm SR}$ is the anomalous dimension in the SR limit. While several numerical studies seemingly support Sak's criterion, [24,28,29] other investigations and theoretical analyses favor the $\sigma_* = 2$ scenario. [30-32]

The problem becomes more subtle for the 2D XY model. In the SR limit, the Mermin–Wagner theorem forbids the formation of a long-range order (LRO) phase. [33] Yet, the model undergoes a BKT transition, entering a quasi-long-range order (QLRO) phase. [15] Applying Sak's criterion to the 2D XY model can be especially nuanced because, rather than a single fixed point, the SR critical behavior is governed by an entire line of fixed points with a temperature-dependent anomalous dimension $\eta(T)$, and the phase transition is of topological type. [11,12,15] Conventional strategies for analyzing the XY model, such as mapping it to Coulomb gas or the sine-Gordon model, [34,35] might fail in the presence of LR interaction. [11] Further-

[†]These authors contributed equally to this work.

^{*}Corresponding authors. Email: zhangchao1986sdu@gmail.com; zfanac@ustc.edu.cn; yjdeng@ustc.edu.cn

^{© 2025} Chinese Physical Society and IOP Publishing Ltd. All rights, including for text and data mining, AI training, and similar technologies, are reserved.

more, the numerical study of this model faces considerable difficulties, including logarithmic corrections owing to BKT universality, $^{[15,36]}$ severe finite-size effects, and the escalating computational costs associated with LR interactions. $^{[37,38]}$

Recent field-theoretical studies of the 2D LR XY model predict an exotic phase diagram. $^{[11,12]}$ An intermediate QLRO phase is stabilized for 1.75 $< \sigma < 2$, below which the system enters an LRO phase. Intriguingly, a similar study on the LR Villain model reveals different behavior, $^{[39]}$ despite both models belonging to the same universality class in the SR limit. $^{[40,41]}$ This deviation is particularly notable given that such an intermediate QLRO phase is absent in previous numerical results of the LR diluted XY model in 2D, $^{[42]}$ a model expected to share the same critical behaviors as the 2D LR XY model. $^{[42,43]}$

In this Letter, we study the 2D LR XY model with power-law decaying $\sim 1/r^{d+\sigma}$ interactions by large-scale simulations up to a linear size of L = 8192. The phase diagram of the model, as depicted in Fig. 1, is characterized by three distinct regimes: the classical ($\sigma \leq 1$), the non-classical (1 $< \sigma \le 2$), and the SR regime ($\sigma > 2$). As expected, for $\sigma < 1$, the critical behaviors are governed by Gaussian mean-field theory, [23] while for $\sigma > 2$, the system exhibits BKT transitions. The non-classical regime $(1 < \sigma \le 2)$ is of particular interest. The finite-size scaling (FSS) behaviors in this regime demonstrate that the system undergoes a second-order transition (Fig. 2). Rather than focusing on refining the estimates of the σ -dependent critical exponents, we investigate the low-T and high-Tproperties of the model. In the low-T phase for $\sigma \leq 2$, we show that the LR ferromagnetic order emerges, i.e., magnetization density M > 0. The two-point correlation function decays as a power law $g(x) \simeq g_0 + cx^{-\eta_\ell}$ and saturates to a constant $g_0 = M^2$, as distance $x \to \infty$. Here, the magnetic anomalous exponent $\eta_{\ell} = 2 - \sigma$ can be theoretically derived from the Goldstone-mode (transverse)

fluctuations of the order parameter. For the marginal case $\sigma = 2$ ($\eta_{\ell} = 0$), logarithmic scaling behaviors are clearly observed, though a theoretical derivation is still lacking. In the high-T paramagnetic phase, the growth behavior of the correlation length ξ is carefully examined as temperature Tdecreases and approaches the critical point T_c . For $\sigma > 2$, ξ grows exponentially as $\sim e^{b/\sqrt{t}}$ with $t \equiv (T - T_c)/T_c$ being the reduced temperature. The data of ξ at different σ collapse on top of each other, clearly illustrating the BKT physics. However, for $\sigma \leq 2$, the growth of ξ deviates more and more from the BKT curve as L increases, and a power-law behavior is asymptotically observed, clearly indicating a second-order phase transition. Strong evidence for $\sigma_* = 2$ is also found by studying the low-T transition from the QLRO phase to the LRO ferromagnet as σ crosses $\sigma = 2$. Finally, we determine with high precision the critical points and critical exponents in the non-classical regime $1 < \sigma \le 2$. More technical details and extensive analysis are presented in Ref. [44].

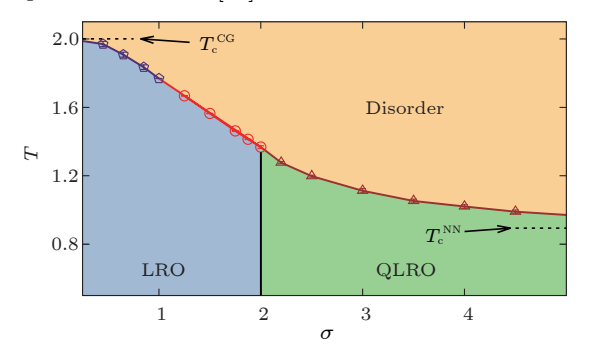


Fig. 1. Phase diagram of the LR XY model in 2D. The SR regime ($\sigma > 2$) exhibits BKT transitions (brown line) into the QLRO phase. In the non-classical regime ($1 < \sigma \le 2$), the system undergoes a second-order transition (red line) into an LRO phase. Finally, in the classical regime ($\sigma \le 1$), the transition (purple lines) is described by the Gaussian theory. Symbol $T_c^{\rm CG}$ stands for the critical temperatures for the complete-graph case and $T_c^{\rm NN}$ for the nearest-neighbor (NN) case.

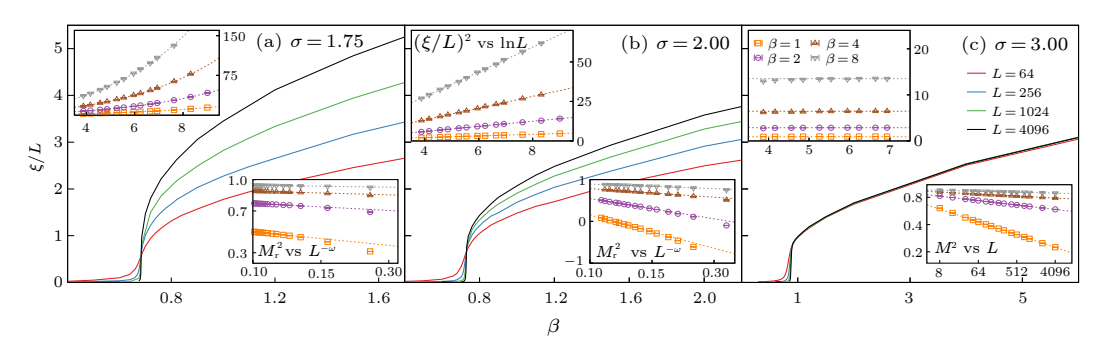


Fig. 2. Emergence of the LRO for $\sigma \leq 2$. As temperature T decreases, the correlation-length ratio ξ/L for (a) $\sigma = 1.75$ and (b) $\sigma = 2$ displays typical scaling behaviors for a system entering into a LR ordered phase via a continuous phase transition at T_c : it has an asymptotically universal value at $T = T_c$ and diverges for $T < T_c$ as L increases. In contrast, for (c) $\sigma = 3$, which has a BKT transition, ξ/L for different L quickly converges to a smooth function for $T < T_c$, as a consequence of the algebraically decaying QLRO. The top left insets illustrate the divergence of $(\xi/L)^2$ in the low-T phase for $\sigma = 1.75$ and 2 compared to the quick convergence for the $\sigma = 3$ case. We find a power-law divergence $(\xi/L)^2 \sim L^{\eta_\ell}$ with a T-independent exponent η_ℓ for $\sigma = 1.75$ and a logarithmic divergence $\sim \ln L$ for the marginal case $\sigma = 2$ (see the text for details). Moreover, the bottom right insets for $\sigma = 1.75$ and 2 plot the residual magnetization density M_r^2 against $L^{-\omega}$, with $\omega = 0.65$ and 0.4, respectively. The extrapolation of M_r^2 converges to positive values in the $L \to \infty$ limit, providing direct evidence for the ferromagnetic order in the low-T phase. In contrast, for $\sigma = 3$, M^2 exhibits an algebraic decay characteristic of a QLRO phase.

2. Model, Algorithm and Observables. We consider the LR interacting XY model on a square lattice of side length L, described by the Hamiltonian $H = -\sum_{i < j} J/r_{i,j}^{d+\sigma} S_i \cdot S_j$, where S_i and S_j are 2-component unit spin vectors at sites i and j, respectively, and $r_{i,j}$ denotes the distance between these sites. The summation encompasses all unique pairs of spins. With periodic boundary conditions, each spin interacts with the other N-1 spins $(N=L^2)$ via the shortest distance. In addition, the interaction strength J is normalized such that $\sum_{j>0} J/r_{0,j}^{2+\sigma} = 4$, to satisfy the strict extensibility of the total energy and thus to reduce unnecessary finite-size corrections. [29,44-46] The Boltzmann weight of a configuration is $\exp(-\beta H)$, with $\beta = 1/k_{\rm B}T$ the inverse temperature $(k_{\rm B}=1)$ is set).

Substantial computational expense is the primary factor hindering large-scale simulations of the model. In conventional Monte Carlo methods, it scales as $\mathcal{O}(N)$ per spin update due to LR interactions. Specialized techniques have been developed to efficiently simulate LR interacting systems. [29,37,38,46] We employ an enhanced version of the Luijten–Blöte algorithm, [37,46] which utilizes cluster spin updates [47,48] alongside an exceedingly efficient cluster construction procedure (see Ref. [44] for details). This technique significantly accelerates the construction of clusters, rendering the computational time per spin independent of N. Specifically, we incorporate the clock sampling technique [38] to efficiently sample bond activation events, substantially improving computational speed and memory usage. It also eliminates the need for a look-up table and alleviates truncation errors stemming from discrete cumulative probability integration approximations. [46]

Various physical quantities are measured. given configuration, we compute the magnetization density $M = L^{-2} |\sum_i \mathbf{S}_i|$, and its Fourier transform $M_k = L^{-2} |\sum_i \mathbf{S}_i e^{i\mathbf{k}\cdot\mathbf{r}_i}|$. Here, \mathbf{r}_i denotes the coordinates of site i and $\mathbf{k} = (2\pi/L, 0)$ is the smallest wave vector along the x-axis. After thermalization, we obtain the susceptibility $\chi = L^2 \langle M^2 \rangle$, the Fourier-transformed susceptibility $\chi_k = L^2 \langle M_k^2 \rangle$, where $\langle \cdot \rangle$ represents the statistical average. We also measure the second-moment correlation length $\xi_{2\text{nd}} = 1/\left[2\sin(|\mathbf{k}|/2)\right]\sqrt{\langle M^2\rangle/\langle M_k^2\rangle-1}$. In the disordered phase, it is asymptotically equivalent to the conventional exponential correlation length ξ_{exp} in the thermodynamic limit, but is much easier to compute as it requires no fitting. At criticality and in the ordered phase, however, their behaviors differ. At the critical point, ξ_{exp} is illdefined due to the algebraically decaying correlation functions, while ξ_{2nd} scales proportionally to the system size L, and the ratio ξ_{2nd}/L converges to a universal value. Similarly, in the QLRO phase, ξ_{2nd}/L converges to a universal function of β . In the ordered phase, ξ_{2nd} diverges due to finite $\langle M^2 \rangle$ and vanishing $\langle M_k^2 \rangle$ in the $L \to \infty$ limit. For the ordered phase without Goldstone mode, ξ_{2nd} typically scales as $\sim L^{1+d/2}$ while $\xi_{\rm exp}$ remains finite. In contrast, in systems with Goldstone modes, ξ_{exp} is again ill-defined, and ξ_{2nd} scales as $\sim L^{1+(2-d+\eta_l)/2}$. Overall, ξ_{2nd} serves as a robust and informative indicator of different phases. [49–53] For brevity, we refer to ξ_{2nd} as ξ throughout this paper.

We use the standard binning and jackknife methods to estimate the error bars.

3. Results. Dimensionless quantities, such as the Binder cumulant [54] and the second-moment correlation length ratio ξ/L , [49-52] are powerful tools for studying phase transitions. Figure 2 shows that for $\sigma \leq 2$, the ξ/L curves display the typical FSS behaviors of a second-order transition, i.e., ξ/L curves of different L share a universal intersection point at $T=T_{\rm c}$ and diverge for $T< T_{\rm c}$ as L increases. [49–52] We perform least-squares fits using the standard FSS technique to accurately estimate the critical points and critical exponents in the non-classical regime $1 \leq \sigma \leq 2$, as presented in Table 1. As a reference, characteristic FSS behavior of BKT transitions is observed for $\sigma = 3$, where ξ/L curves converge to a nontrivial smooth function and no finite magnetization develops for $T \leq T_c$. [15,55] These results suggest a threshold value $\sigma_* = 2$ in the LR XY model, below which the system develops a LR order parameter and becomes a ferromag-

The spontaneous O(2) symmetry breaking for $\sigma \leq 2$ naturally implies the existence of Goldstone mode in the low-T phase. Consider the field-theoretical Hamiltonian of 2D LR $O(\mathcal{N})$ models in momentum-space,

$$\beta H = \int \frac{\mathrm{d}^2 q}{(2\pi)^2} \left(\frac{K_2}{2} q^2 + K_\sigma q^\sigma \right) \Psi(\mathbf{q}) \cdot \Psi(-\mathbf{q}) + \int \mathrm{d}^2 x \left(\frac{t}{2} \Psi^2 + u \Psi^4 \right) , \tag{1}$$

where Ψ is the \mathcal{N} -component order parameter field, t is the distance to criticality, and K_2 , K_{σ} , u are coupling constants. In the low-T phase (t < 0), when a LRO exists, the system is far from criticality, and renormalization becomes trivial; thus, for $\sigma < 2$, $K_{\sigma}q^{\sigma}$ becomes the leading term, and $\frac{K_2}{2}q^2$ can be ignored. Employing the saddle point approximation, Ψ can then be written in terms of longitudinal and transverse (Goldstonemode) fluctuations $\Psi(x) = \Psi_{L}(x) + \Psi_{T}(x)$. In this expansion, the two-point correlation of transverse fluctuation in momentum space $\langle \Psi_{\rm T}(\boldsymbol{q})\Psi_{\rm T}(-\boldsymbol{q})\rangle$ is proportional to $|q|^{-\sigma}$, which results in a power-law correlation in realspace $\langle \Psi_{\rm T}(0)\Psi_{\rm T}(\boldsymbol{x})\rangle \sim |\boldsymbol{x}|^{-2+\sigma}$. Therefore, for the LR XY model, one has $g(x) = g_0 + cx^{-\eta_\ell}$, where $\eta_\ell = 2 - \sigma$ and c is a constant. Accordingly, one can derive in the LRO phase for $\sigma < 2$, $M^2 \sim M_0^2 + bL^{-\eta_\ell}$, $\chi_k \sim L^{2-\eta_\ell}$ and $\xi \sim L^{1+\eta_\ell/2}$. In the marginal case of $\sigma=2$, however, the exact scaling form of q(x) is not straightforward to

Table 1. Critical point β_c and critical exponents of LR XY model for various σ in the non-classical regime. Here, ν is the correlation length exponent, and η is the magnetic anomalous dimension. In the low-T phase, η_ℓ is consistent with theoretical prediction, $\eta_\ell = 2 - \sigma$.

σ	$eta_{ m c}$	$1/\nu$	η	η_ℓ
1.250	0.599615(6)	0.987(4)	0.75(1)	0.751(2)
1.750	0.68380(7)	0.60(4)	0.324(7)	0.250(2)
1.875	0.70737(7)	0.48(4)	0.278(5)	0.122(5)
2.000	0.7315(2)	0.37(4)	0.260(5)	$0 (1/\ln L)$

derive. Nevertheless, it is natural to expect logarithmic corrections as the anomalous dimension η_{ℓ} vanishes and the LR and SR terms become degenerate. [56,57] Hence, we conjecture that, at $\sigma=2$, $M^2\sim M_0^2+\ln(L/L_0)^{\hat{\eta}_{\ell}}$, $\chi_k\sim L^2\ln(L/L_0')^{\hat{\eta}_{\ell}}$ and $\xi\sim L\ln(L/L_0'')^{-\hat{\eta}_{\ell}/2}$. Here, $\hat{\eta}_{\ell}$ is the exponent of the logarithmic correction, and L_0 , L_0' , L_0'' are non-universal constants.

The upper-left insets of Fig. 2, showing $(\xi/L)^2$ as a function of $\ln L$, demonstrate distinctive low-T scaling behaviors of ξ/L for different σ values. For $\sigma=2$, the data points can be well-described by straight lines of $\ln L$, which confirms the conjectured logarithmic scaling behavior and indicates $\hat{\eta}_\ell=-1$, i.e., $(\xi/L)^2\sim \ln L$. For $\sigma=1.75$, the bending-up curvatures mean that divergences of ξ/L are faster than the logarithmic growth. The least-squares fit by $(\xi/L)^2=c+L^{\eta_\ell}(a+bL^{-1})$, with constants a,b, and c, gives $\eta_\ell=0.250(4)$ for various T values, well consistent with the theoretical prediction. Fitted values of η_ℓ are given in Table 1. By contrast, for $\sigma=3$, ξ/L quickly converges to a constant with increasing L.

Direct evidence of LRO for $\sigma \leq 2$ and $T < T_{\rm c}$ is presented in the bottom-right insets of Fig. 2 by showing the low-T scaling behavior of the residual magnetization $M_{\rm r}^2$. FSS analysis of M^2 suffers from strong finite-size corrections from Goldstone-mode fluctuations; such corrections can be reduced by defining a residual magnetization $M_{\rm r}^2 = M^2 - bM_k^2$, where b > 0 is some constant.^[44] By definition, M_k^2 is a lower bound of M^2 , i.e., $M_k^2 \leq M^2$, and the extrapolation of $M_{\rm r}^2$ in the thermodynamic limit converges faster than that of M^2 . For $\sigma = 1.75$ and 2, M_r^2 versus $L^{-\omega}$, with $\omega = 0.65$ and 0.4 respectively, clearly extrapolates to positive values, illustrating an LRO phase. Here, b = 22 for all β for $\sigma = 1.75$ and b = 149, 175, 152, and 154 for $\beta = 1, 2, 4$, and 8 in $\sigma = 2$. It is further noted that the correction amplitude of $L^{-\omega}$ in M_r^2 is negative, and the value of $M_{\rm r}^2$ is already positive for finite Ls, strongly indicating that in the $L \to \infty$ limit $M_{\rm r}^2 > 0$ and consequently $M^2 > 0$. Our results provide compelling evidence that as long as $\sigma \leq 2$, the LR XY model enters a ferromagnetic phase and thus, the phase transition should be of the second order. Note that our findings differ from those of Refs. [11,12].

We now turn to the high-T properties at $\sigma = 2$, specifically the growth of the second-moment correlation length ξ as T approaches T_c from above. [53] In the context of RG, near a BKT fixed point, ξ exhibits an exponential divergence, $\xi \sim \exp(b/\sqrt{t})$, where t is the reduced temperature $t = (T - T_c)/T_c$ and b is a non-universal constant. [36] Conversely, ξ diverges algebraically, $\xi \sim t^{-\nu}$, near a secondorder transition. We first determine the critical points $T_c(\sigma = 2) = 1.3671(4)$ and $T_c(\sigma = 3) = 1.109(2)$, then plot ξ of various L against b/\sqrt{t} on a semi-log scale for $\sigma=2,3,$ and the NN case (Fig. 3). Note that for given ts, ξ quickly converges to its thermodynamic value as L increases, except when $t \to 0$ and the system enters the finite-size critical window, where $\xi \sim L$ and the curve bends to a plateau. For $\sigma = 3$ and the NN case, the thermodynamic values of ξ collapse onto a single linear trajectory, consistent with the BKT behavior. For $\sigma=2$, however, as t decreases, the growth behavior of ξ increasingly deviates from the BKT curves, suggesting a different universality class. Furthermore, the log-log plot in the inset shows that for $\sigma=2$, ξ asymptotically follows an algebraic scaling (visually approximated by $t^{-2.22}$). The deviation from the FSS fitting result is due to strong finite-size corrections at $\sigma=2$; the exponent of the power-law growth should asymptotically converge to $\nu=2.7(3)$ as the system size further increases and t decreases. Nevertheless, these results strongly suggest that instead of being BKT-type, the phase transition at $\sigma=2$ is a second-order transition.

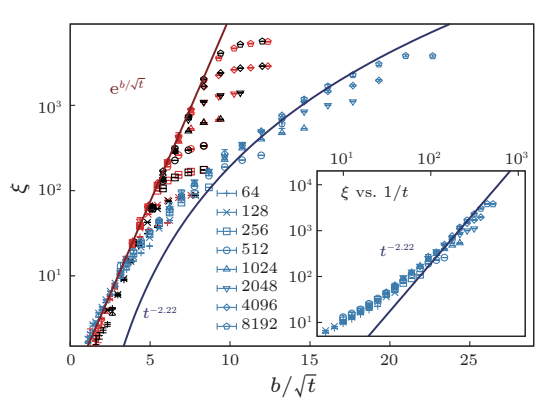


Fig. 3. Deviation of correlation length growth at $\sigma=2$ from the BKT scaling. The main panel shows a semi-logarithmic plot of ξ as a function of b/\sqrt{t} for various L at $\sigma=2$ (blue dots), 3 (red dots), and NN XY case (black dots), where t is the reduced temperature, and b=1, 1.25, and 1.625 respectively. For the $\sigma=3$ and NN XY case, the linear behavior of ξ demonstrates an exponential growth of ξ , characterizing the BKT transition. However, for $\sigma=2$, the growth of ξ deviates more and more from the BKT behavior as the system approaches the critical point. The inset shows a double-log plot of ξ versus 1/t for $\sigma=2$, revealing a power-law behavior of ξ , thus highlighting the second-order phase transition.

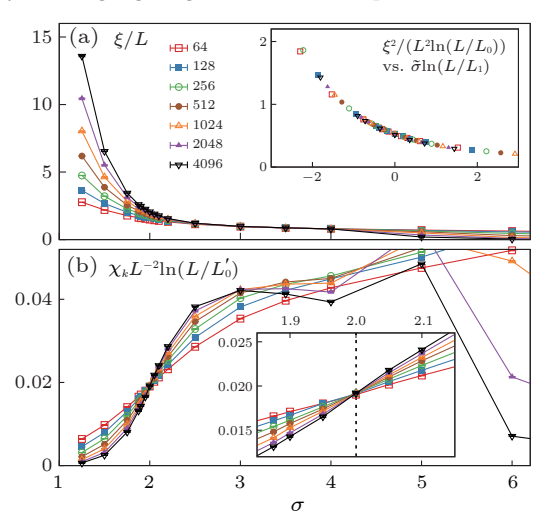


Fig. 4. Low-T transitions at $\sigma=2$ with T=1. (a) ξ/L versus σ for various L. The system enters the LRO phase when $\sigma\leq 2$. The inset shows good data collapse of $\xi/(L\ln(L/L_0)^{1/2})$ versus $\tilde{\sigma}\ln(L/L_1)$, where $\tilde{\sigma}=\sigma-2$, $L_0=2.9$ and $L_1=3$. (b) $\chi_k L^{-2}\ln(L/L'_0)$ versus σ for various L, with $L'_0=2.9$. The scaled χ_k curves have a clear crossing point at $\sigma=2$ as demonstrated in both panel (b) and its inset.

Previous analysis demonstrates logarithmic behaviors of ξ/L and χ_k in the low-T phase at $\sigma=2$. Here, we fix the temperature at T=1.0, which is below the critical point $T_{\rm c}(\sigma=2)=1.3671(4)$ but sufficiently high, and study the behaviors of ξ and χ_k as a function of σ . Figure 4(a) shows three phases as σ decreases. The system first enters the QLRO phase from the disordered phase via a BKT transition at $\sigma \approx 4.0$; as σ further declines, ξ/L curves begin diverging near $\sigma = 2$, indicating the transition into LRO phases. We also plot $\chi_k L^{-2} \ln(L/L'_0)$ as a function of σ for various L in Fig. 4(b), with a constant $L'_0 = 2.9$. These curves exhibit an intersection at $\sigma = 2$, consistent with theoretical predictions. A zoomed-in plot in the inset better displays this crossing. Moreover, considering the logarithmic corrections at $\sigma = 2$ and $T < T_c$, we conjecture the scaling of ξ near $\sigma = 2$ as $\xi = L \ln(L/L_0)^{\frac{1}{2}} \xi' [\tilde{\sigma} \ln(L/L_1)],$ where $\tilde{\sigma} = \sigma - 2$, $\xi'[\cdot]$ is a universal scaling function, and L_0 and L_1 are non-universal constants. As shown in the inset, the scaled ξ data points collapse onto the same curve, further supporting the $\sigma_* = 2$ scenario. It is noteworthy that, in the thermodynamic limit, the magnetization density is finite in the LRO phase while vanishing in the QLRO phase, which should manifest a first-order-like discontinuity at $\sigma = 2$.

4. Conclusion and Outlook. Our study reveals that, for $\sigma \leq 2$, the 2D LR XY model enters a ferromagnetic phase at low-T through a second-order transition, indicating the threshold value at $\sigma_* = 2$. We show that the system exhibits finite magnetization density and Goldstone mode fluctuation in the low-T phase. The power-law growth of ξ near the critical point further demonstrates that the phase transition at $\sigma = 2$ is the second-order, excluding the scenario predicted in Ref. [11]. Finally, for $\sigma = 2$ and $T < T_c$, the observed multiplicative logarithmic behavior requires further theoretical investigation.

Preliminary investigations for the 2D LR Heisenberg model illustrate that the algebraic interaction would induce a LR ordered ferromagnet as long as $\sigma \leq 2$; while the system exhibits no finite-T transition for $\sigma > 2$. Ongoing studies are being conducted for a systematic revisit of the LR $O(\mathcal{N})$ spin models, including the Ising model that has been extensively studied in literatures. The success of this work also suggests that, instead of simply improving over the estimate of critical exponents, one can study the system in an extended parameter space, e.g., the geometric structures of the Ising model and the selfavoiding random walk, which corresponds to the $\mathcal{N} \to 0$ limit of the $O(\mathcal{N})$ spin model. [58] In addition, the topology of our phase diagram differs from that of the LR quantum XXZ chain, [12,59] which implies that the direct mapping [60] might be invalid here, posing an open question about the correspondence between LR classical and LR quantum models. Finally, we emphasize that our work may be of timely application in cutting-edge experiments, such as trapped ions and Rydberg-atom arrays, that involve LR interactions.

Acknowledgments. We thank Sheng Fang for initiating this project. YD thanks N. Defenu for valuable discussions, who pointed out that higher-order terms were omitted in the theoretical derivation in Ref. [11]. This work

was supported by the National Natural Science Foundation of China (Grant Nos. 12204173 and 12275263), and the Innovation Program for Quantum Science and Technology (Grant No. 2021ZD0301900). YD is also supported by the Natural Science Foundation of Fujian Province 802 of China (Grant No. 2023J02032).

References

- [1] Spivak B and Kivelson S A 2004 Phys. Rev. B 70 155114
- [2] Lahaye T, Menotti C, Santos L, Lewenstein M, and Pfau T 2009 Rep. Prog. Phys. 72 126401
- [3] Peter D, Müller S, Wessel S, and Büchler H P 2012 Phys. Rev. Lett. 109 025303
- [4] Saffman M, Walker T G, and Mølmer K 2010 Rev. Mod. Phys. 82 2313
- [5] Lu M W, Burdick N Q, and Lev B L 2012 Phys. Rev. Lett. 108 215301
- [6] Schauß P, Cheneau M, Endres M, Fukuhara T, Hild S, Omran A, Pohl T, Gross C, Kuhr S, and Bloch I 2012 Nature 491 87
- [7] Firstenberg O, Peyronel T, Liang Q Y, Gorshkov A V, Lukin M D, and Vuletic V 2013 Nature 502 71
- [8] Yan B, Moses S A, Gadway B, Covey J P, Hazzard K R A, Rey A M, Jin D S, and Ye J 2013 Nature 501 521
- [9] Aikawa K, Frisch A, Mark M, Baier S, Rietzler A, Grimm R, and Ferlaino F 2012 Phys. Rev. Lett. 108 210401
- [10] Lewis D, Banchi L, Teoh Y H, Islam R, and Bose S 2023 Quantum Sci. Technol. 8 035025
- [11] Giachetti G, Defenu N, Ruffo S, and Trombettoni A 2021 Phys. Rev. Lett. 127 156801
- [12] Giachetti G, Trombettoni A, Ruffo S, and Defenu N 2022 Phys. Rev. B 106 014106
- [13] Chen C, Bornet G, Bintz M, Emperauger G, Leclerc L, Liu V S, Scholl P, Barredo D, Hauschild J, Chatterjee S, Schuler M, Läuchli A M, Zaletel M P, Lahaye T, Yao N Y, and Browaeys A 2023 Nature 616 691
- [14] Chen X Y, Schindewolf A, Eppelt S, Bause R, Duda M, Biswas S, Karman T, Hilker T, Bloch I, and Luo X Y 2023 Nature 614 59
- [15] Kosterlitz J M 2017 Rev. Mod. Phys. 89 040501
- [16] Bishop D J and Reppy J D 1978 Phys. Rev. Lett. 40 1727
- [17] Epstein K, Goldman A M, and Kadin A M 1981 Phys. Rev. Lett. 47 534
- [18] Benfatto L, Castellani C, and Giamarchi T 2007 Phys. Rev. Lett. 98 117008
- [19] Fazio R 2001 Phys. Rep. **355** 235
- [20] Kunz H and Pfister C E 1976 Commun. Math. Phys. 46 245
- [21] Fisher M E, Ma S k, and Nickel B G 1972 Phys. Rev. Lett. 29 917
- [22] Sak J 1973 Phys. Rev. B 8 281
- [23] Defenu N, Donner T, Macrì T, Pagano G, Ruffo S, and Trombettoni A 2023 Rev. Mod. Phys. 95 035002
- [24] Angelini M C, Parisi G, and Ricci-Tersenghi F 2014 Phys. Rev. E 89 062120
- [25] Brezin E, Parisi G, and Ricci-Tersenghi F 2014 J. Stat. Phys. 157 855
- [26] Defenu N, Trombettoni A, and Ruffo S 2017 Phys. Rev. B 96 104432
- [27] Defenu N, Trombettoni A, and Codello A 2015 Phys. Rev. E ${\bf 92}$ 052113
- [28] Luijten E and Blöte H W J 2002 Phys. Rev. Lett. 89 025703
- [29] Horita T, Suwa H, and Todo S 2017 Phys. Rev. E 95 012143
- [30] van Enter A C D 1982 Phys. Rev. B 26 1336

- [31] Grassberger P 2013 J. Stat. Phys. 153 289
- [32] Blanchard T, Picco M, and Rajabpour M A 2013 Europhys. Lett. 101 56003
- [33] Mermin N D and Wagner H 1966 Phys. Rev. Lett. 17 1133
- [34] Minnhagen P 1987 Rev. Mod. Phys. 59 1001
- [35] Gulácsi Z and Gulácsi M 1998 Adv. Phys. Adv. Phys. 47
- [36] Chen H, Hou P C, Fang S, and Deng Y J 2022 Phys. Rev. E: Stat. Phys. Plasmas Fluids 106 024106
- [37] Luijten E and Blöte H W 1995 Int. J. Mod. Phys. C 06 359
- [38] Michel M, Tan X J, and Deng Y J 2019 Phys. Rev. E: Stat. Phys. Plasmas Fluids 99 010105
- [39] Giachetti G, Defenu N, Ruffo S, and Trombettoni A 2023 J. High. Energy Phys. 2023 238
- [40] Villain J 1975 Journal de Physique 36 581
- [41] José J V, Kadanoff L P, Kirkpatrick S, and Nelson D R 1977 Phys. Rev. B 16 1217
- [42] Cescatti F, Ibáñez-Berganza M, Vezzani A, and Burioni R 2019 Phys. Rev. B 100 054203
- [43] Berganza M I and Leuzzi L 2013 Phys. Rev. B 88 144104
- $[44]\ \, {\rm Yao}\ \, {\rm D}\ \, {\rm Y},\, {\rm Xiao}\ \, {\rm T}\ \, {\rm N},\, {\rm Zhang}\ \, {\rm C},\, {\rm Fan}\ \, {\rm Z}\ \, {\rm J}\ \, {\rm and}\ \, {\rm Deng}\ \, {\rm Y}\ \, {\rm J}\ \, 2024$ ${\rm arxiv}:2411.01811$
- [45] Filinov A, Prokof'ev N V, and Bonitz M 2010 Phys. Rev. Lett. 105 070401

- [46] Luijten E and Blote H W J 1997 Phys. Rev. B 56 8945
- [47] Swendsen R H and Wang J S 1987 Phys. Rev. Lett. 58 86
- [48] Wolff U 1989 Phys. Rev. Lett. 62 361
- [49] Viet D X and Kawamura H 2009 Phys. Rev. B 80 064418
- [50] Ding C X, Guo W A, and Deng Y J 2014 Phys. Rev. B 90 134420
- [51] Komura Y and Okabe Y 2012 J. Phys. Soc. Jpn. 81 113001
- [52] Surungan T, Masuda S, Komura Y, and Okabe Y 2019 J. Phys. A: Math. Theor. 52 275002
- [53] Yao D Y, Zhang C, Xie Z Y, Fan Z J, and Deng Y J 2025 2503.2 4226 arXiv:2503.24226 [cond-mat.stat-mech]
- [54] Binder K 1981 Zeitschrift fur Physik B Condensed Matter 43 119
- [55] Tuan L M, Long T T, Nui D X, Minh P T, Trung Kien N D, and Viet D X 2022 Phys. Rev. E 106 034138
- [56] Wegner F J 1972 Phys. Rev. B 5 4529
- [57] Wegner F J and Riedel E K 1973 Phys. Rev. B 7 248
- [58] Fang S, Deng Y J, and Zhou Z Z 2021 Phys. Rev. E 104 064108
- [59] Maghrebi M F, Gong Z X, and Gorshkov A V 2017 Phys. Rev. Lett. 119 023001
- [60] Mattis D C 1984 Phys. Lett. A 104 357